PHYSICAL REVIEW B VOLUME 25, NUMBER 2 15 JANUARY 1982

Energy- and stress-dependent hole masses in germanium and silicon

S. M. Kelso*
Physics Department, University of California and Materials and Molecular Research Division, Lawrence Berkeley Laboratory, Berkeley, California 94720 and Bell Laboratories, Murray Hill, New Jersey 07974
(Received 8 June 1981)

We present calculated results for several energy- and stress-dependent hole masses for uniaxial ⟨001⟩, ⟨111⟩, and ⟨110⟩ stresses in Ge and Si: local and integrated density-of-states masses and longitudinal and transverse optical-mass components for the valence bands corresponding to $|M_J|=\frac{1}{2}$ and $\frac{3}{2}$. These masses depend on energy E and stress σ through the form $m(E,\sigma)=m(E/\sigma)$. The masses will be useful in the analysis of experimental luminescence and plasma absorption line shapes, as well as in the calculation of other properties of electron-hole liquids in stressed Ge and Si.

I. INTRODUCTION

Over the last several years there has been much interest in the electron-hole liquid[1] (EHL) in stressed Ge and Si. A primary motivation for this interest is the fact that the band structure of Ge (Si) simplifies considerably under infinite uniaxial ⟨111⟩ (⟨001⟩) compression, thus making theories more tractable. From the experimental point of view, properties of the EHL for infinite stress must of course be inferred from measurements at finite stress. There is also considerable interest in the variation of EHL properties with stress at moderate stresses, where the band structure is more complex than for either zero or infinite stress.

The experimental probe most widely used to study electron-hole liquids is the characteristic (near-infrared) luminescence emitted as electron-hole pairs recombine.[1] Another experimental probe, less widely used, is the far-infrared plasma absorption of the electrons and holes.[1] In both types of experiment a proper line-shape analysis requires a description of the structure of the valence bands. This is particularly true at intermediate stresses, where the bands interact strongly. An accurate description of the valence bands may be conveniently obtained through the use of appropriately defined masses.[2] For example, the luminescence line shape uses a density-of-states mass, while the plasma absorption line shape uses a plasma or optical mass. In stressed Ge or Si these masses are functions of both energy E and stress σ, but the dependences are not separate: $m(E,\sigma)=m(E/\sigma)$.

In this paper we present calculations of local and integrated density-of-states masses as well as longitudinal and transverse optical-mass components for the valence bands of Ge and Si stressed along each of the principal crystallographic directions ⟨001⟩, ⟨110⟩, and ⟨111⟩. The local density-of-states masses for ⟨111⟩-stressed Ge have been published previously[3] and are repeated here for completeness. Liu[4] showed partial results for an energy-dependent integrated density-of-states mass for two values of ⟨111⟩ stress in Ge and ⟨001⟩ stress in Si, apparently not recognizing the scaling relation. Kirczenow and Singwi[5] gave results for a quantity related to an integrated density-of-states mass averaged over both bands for ⟨111⟩ stress in Ge. One motivation for presenting the masses explicitly is to provide the necessary tools to experimentalists for EHL line-shape analyses in uniaxially stressed Ge and Si. In addition, the masses are used in the calculation of other properties of electron-hole liquids in stressed semiconductors.[2,4–9]

The calculation of the density-of-states and optical masses is outlined in Sec. II. Results are presented in Sec. III for the three principal stress directions in Ge and Si. One use of the masses for the analysis of luminescence line shapes is illustrated in Sec. IV.

II. THEORY

We begin by summarizing the valence-band structure near $\vec{k}=0$ for strained Ge and Si, as calculated using the $\vec{k}\cdot\vec{p}$ formalism by Pikus and Bir.[10] The valence-band dispersion is given by[10,11]

 ©1982 The American Physical Society

$$E(k)=Ak^2+|E_{\epsilon\epsilon}|\pm(E_{kk}^2+E_{\epsilon k}^2+E_{\epsilon\epsilon}^2)^{1/2}\ , \tag{1a}$$

where

$$E_{kk}^2=B^2k^4+C^2(k_x^2k_y^2+\text{c.p.}) \tag{1b}$$

$$E_{\epsilon k}^2=Bb[3(k_x^2\epsilon_{xx}+\text{c.p.})-k^2\Delta]+2Dd(k_xk_y\epsilon_{xy}+\text{c.p.}) \tag{1c}$$

$$E_{\epsilon\epsilon}^2=\tfrac{1}{2}b^2[(\epsilon_{xx}-\epsilon_{yy})^2+\text{c.p.}]+d^2(\epsilon_{xy}^2+\text{c.p.})\ . \tag{1d}$$

Here A, B, and C are inverse-mass band parameters,[12] $D=(3B^2+C^2)^{1/2}$, b and d are deformation potentials, the ϵ_{ij} are strain components, $\Delta=\epsilon_{xx}+\epsilon_{yy}+\epsilon_{zz}$, and c.p. indicates cyclic permutation of the crystal coordinates x, y, and z. The two bands are warped due to the mixing which arises from the degeneracy at $\vec{k}=0$ at zero stress. At infinite stress the bands are completely decoupled and are given by simple ellipsoids. However, as will be seen below, the residual nonparabolicity remains important at stresses much greater than those required to merely depopulate the upper band.

A comment is in order on the labeling of the two bands. At zero stress the designations heavy and light, determined by the relative curvature, are conventional. Under compressive stresses the light-hole band moves "through" the heavy-hole band,[13,14] resulting in strong mixing. For high stresses it is more appropriate to label the bands by the quantum number $|M_J|$, where $|M_J|=\frac{1}{2}$ or $\frac{3}{2}$. This labeling is exact (at $\vec{k}=0$) for $\langle 001\rangle$ and $\langle 111\rangle$ stresses. For $\langle 110\rangle$ stress the $|M_J|=\frac{1}{2}$ and $\frac{3}{2}$ states are in general mixed, but the designation is still approximately correct if the splitting anisotropy parameter β, defined below, is not too different from 1. This is the case for Ge and Si. Here we shall label the masses with the most appropriate quantum number $|M_J|$. Thus the lower sign in Eq. (1a) corresponds to $|M_J|=\frac{1}{2}$ (heavy hole at zero stress). This band remains populated at all stresses. The upper sign then corresponds to the $|M_J|=\frac{3}{2}$ band (light hole at zero stress), which becomes depopulated at high stress.

The strain components ϵ_{ij} in Eq. (1) are given by Hensel and Feher[13] for stresses along the principal crystallographic directions with the x, y, and z crystal coordinates along (100) directions. Thus Eqs. (1c) and (1d) may be simplified as follows:

$$\left.\begin{aligned}E_{\epsilon\epsilon}&=b\sigma_{001}/(C_{11}-C_{12})\\E_{\epsilon k}^2&=BE_{\epsilon\epsilon}(3k_z^2-k^2)\end{aligned}\right\}\langle 001\rangle\text{ stress}\ , \tag{2a}$$

$$\left.\begin{aligned}E_{\epsilon\epsilon}&=d\sigma_{111}/(2\sqrt{3}C_{44})\\E_{\epsilon k}^2&=\frac{2}{\sqrt{3}}DE_{\epsilon\epsilon}(k_xk_y+\text{c.p.})\end{aligned}\right\}\langle 111\rangle\text{ stress}\ , \tag{2b}$$

$$\left.\begin{aligned}E_{\epsilon\epsilon}&=\left[\frac{b^2}{4(C_{11}-C_{12})^2}+\frac{d^2}{16C_{44}^2}\right]^{1/2}\sigma_{110}\\E_{\epsilon k}^2&=\left[\frac{Bb(k^2-3k_z^2)}{2(C_{11}-C_{12})}-\frac{Ddk_xk_y}{2C_{44}}\right]\sigma_{110}\end{aligned}\right\}\langle 110\rangle\text{ stress}\ , \tag{2c}$$

where σ_{klm} is the stress along the $\langle klm\rangle$ crystallographic direction and the C_{ij} are stiffness constants.[15] Values for the inverse-mass band parameters, deformation potentials, and stiffness constants for Ge and Si are listed in Table I. Also given is the energy splitting $E_{\text{spl}}^h=2|E_{\epsilon\epsilon}|$ between the $|M_J|=\frac{1}{2}$ and $\frac{3}{2}$ bands at $\vec{k}=0$ normalized by the stress for each of the principal stress directions. Note that compressional stresses are negative and are expressed in kgf/mm^2, where 1 kgf=9.806 65 newtons.

Consider next the density of states for a single band of carriers:

$$D(E)=\frac{V}{4\pi^3}\int k^2\frac{dk}{dE}d\Omega\ , \tag{3}$$

where the integration is performed over solid angle on the $\vec{k}$-space surface with energy E. If the band is parabolic, $E(k)=\hbar^2k^2/2m_d$ for a density-of-states mass m_d, then Eq. (3) reduces to a well-known simple form:

$$D(E)=\frac{\sqrt{2}V}{\pi^2\hbar^3}m_d^{3/2}E^{1/2}\ . \tag{4a}$$

If the band is not parabolic, the nonparabolicity can be taken into account by writing

$$D(E)=\frac{\sqrt{2}V}{\pi^2\hbar^3}m_{d\,\text{loc}}^{3/2}(E)E^{1/2}\ . \tag{4b}$$

Thus, the nonparabolicity may be described via an energy-dependent local density-of-states mass:

$$m_{d\,\text{loc}}^{3/2}(E)\equiv\frac{\hbar^3}{4\sqrt{2}\pi E^{1/2}}\int k^2\frac{dk}{dE}d\Omega\ . \tag{5}$$

This local density-of-states mass should be used for calculations of any quantities involving the density of states at finite temperature,[7,9] such as the EHL luminescence line shape (see Sec. IV). For example, the number of carriers N is given by

$$N=\int_0^\infty D(E)(1+e^{[E-E_F(T)]/kT})^{-1}dE\ , \tag{6}$$

TABLE I. Values for parameters used in the calculation of hole masses.

Parameter	Unit	Ge	Ref.	Si	Ref.
A		13.38	a,b	4.28	c
B		8.48	a,b	0.75	c
C		13.14	a,b	4.85	d
b	eV	2.21	a,e	1.36	c,e
d	eV	4.40	a,e	3.09	c,e
C_{11}	kgf/mm^2	13360	f	17100	g
C_{12}	kgf/mm^2	4996	f	7093	g
C_{44}	kgf/mm^2	7016	f	8180	g
$-E^h_{\text{spl}}/\sigma_{001}$	meV mm^2/kgf	0.528	h	0.272	h
$-E^h_{\text{spl}}/\sigma_{111}$	meV mm^2/kgf	0.362	h	0.218	h
$-E^h_{\text{spl}}/\sigma_{110}$	meV mm^2/kgf	0.410	h	0.233	h

[a] J. C. Hensel and K. Suzuki, Phys. Rev. B 9, 4219 (1974).
[b] Reference a gives values for γ_1, γ_2, and γ_3 where $A=-\gamma_1$, $B=-2\gamma_2$, and $C^2=12(\gamma_3^2-\gamma_2^2)$. The signs of A and B are changed here to make the hole band energies positive.
[c] J. C. Hensel and G. Feher, Phys. Rev. 129, 1041 (1963).
[d] J. C. Hensel's experimental value, quoted in P. Lawaetz, Phys. Rev. B 4, 3460 (1971).
[e] References a and c give values for D_u and D_u', where $b=-2D_u/3$ and $d=-2D_u'/\sqrt{3}$. The signs are again changed here to make the energies $E(k)$ positive.
[f] M. E. Fine, J. Appl. Phys. 26, 862 (1965) for $T=1.7$ K.
[g] H. J. McSkimin, J. Appl. Phys. 24, 988 (1953). The data were extrapolated to liquid helium temperatures from 78 K by multiplying by 1.002, a factor obtained by comparison with data for Ge in Ref. f.
[h] $E^h_{\text{spl}}=2\,|E_{\epsilon\epsilon}|$, where $E_{\epsilon\epsilon}$ is given by Eq. (2) for stresses along the principal crystallographic directions.

where $E_F(T)$ is the Fermi energy at temperature T.

For $T=0$ such integrals simplify as the Fermi function becomes a step function. In this case it is convenient to introduce a second density-of-states mass. For example, Eq. (6) becomes

$$N=\frac{2^{3/2}V}{3\pi^2\hbar^3}[E_F(0)]^{3/2}m_{d\,\text{int}}^{3/2}(E_F(0)) , \quad (7)$$

where the integrated density-of-states mass is defined by:

$$m_{d\,\text{int}}^{3/2}(E)\equiv\tfrac{3}{2}E^{-3/2}\int_0^E m_{d\,\text{loc}}^{3/2}(u)u^{1/2}du . \quad (8)$$

Of course, for a parabolic band $m_{d\,\text{int}}(E)=m_{d\,\text{loc}}(E)=\text{const.}$

For calculations involving the dielectric function, optical or conductivity masses should be used.[16] These have been defined by Lax and Mavroides[17] as follows for a single band:

$$\frac{n}{m_{ij}(E)}=\frac{1}{4\pi^3\hbar^2}\int\frac{\partial E}{\partial k_i}\frac{\partial E}{\partial k_j}\frac{\partial k}{\partial E}k^2d\Omega . \quad (9)$$

Here $n=N/V$ is the number of carriers per unit volume, i and j are crystal coordinates x, y, and z, which are along $\langle 100\rangle$ directions, and the integration is again performed over the $\vec{k}$-space surface with energy E. Transverse and longitudinal mass components can be defined, with respect to the stress direction, for stresses along the primary crystallographic directions:

$$\left.\begin{aligned}m_{ol}^{-1}&=m_{zz}^{-1}\\ m_{ot1}^{-1}&=m_{xx}^{-1}\\ m_{ot2}^{-2}&=m_{yy}^{-1}\end{aligned}\right\}\langle 001\rangle \text{ stress} , \quad (10a)$$

$$\left.\begin{aligned}m_{ol}^{-1}&=\tfrac{1}{3}(m_{xx}^{-1}+m_{yy}^{-1}+m_{zz}^{-1})+\tfrac{2}{3}(m_{xy}^{-1}+m_{yz}^{-1}+m_{zy}^{-1})\\ m_{ot1}^{-1}&=\tfrac{1}{2}(m_{xx}^{-1}+m_{yy}^{-1})-m_{xy}^{-1}\\ m_{ot2}^{-1}&=\tfrac{1}{6}[m_{xx}^{-1}+m_{yy}^{-1}+2m_{xy}^{-1}+4(m_{zz}^{-1}-m_{yz}^{-1}-m_{zx}^{-1})]\end{aligned}\right\}\langle 111\rangle \text{ stress} , \quad (10b)$$

$$\left.\begin{array}{l} m_{ol}^{-1}=\frac{1}{2}(m_{xx}^{-1}+m_{yy}^{-1})-m_{xy}^{-1} \\ m_{ot1}^{-1}=\frac{1}{2}(m_{xx}^{-1}+m_{yy}^{-1})+m_{xy}^{-1} \\ m_{ot2}^{-1}=m_{zz}^{-1} \end{array}\right\} \langle 110 \rangle \text{ stress .} \tag{10c}$$

For the $\langle 001 \rangle$ and $\langle 111 \rangle$ directions $m_{ot1}=m_{ot2}$, while for the $\langle 110 \rangle$ direction these transverse components differ. An overall transverse mass is defined via

$$m_{ot}^{-1}=\frac{1}{2}(m_{ot1}^{-1}+m_{ot2}^{-1}) . \tag{11}$$

The above components are combined to give the optical mass for band $|M_J|$:

$$m_{o|M_J|}^{-1}=\frac{1}{3}(2m_{ot}^{-1}+m_{ol}^{-1}) . \tag{12}$$

The overall hole optical mass m_{oh} is obtained from the individual band optical masses, as follows:

$$\frac{n}{m_{oh}}=\sum_{|M_J|}\frac{n_{|M_J|}}{m_{o|M_J|}} , \tag{13}$$

where $\sum_{|M_J|} n_{|M_J|}=n$.

Finally, note that for infinite stress the valence bands become ellipsoidal and thus can be completely characterized by longitudinal and transverse components. For the valence-band dispersion given by Eq. (1), the mass components reduce to the following simple forms[13]:

$$\left.\begin{array}{l} m_l/m_0=(A+B)^{-1} \\ m_{t1}/m_0=m_{t2}/m_0=(A-B/2)^{-1} \end{array}\right\} \text{infinite } \langle 001 \rangle \text{ stress ,} \tag{14a}$$

$$\left.\begin{array}{l} m_l/m_0=\left[A+\dfrac{D}{\sqrt{3}}\right]^{-1} \\ m_{t1}/m_0=m_{t2}/m_0=\left[A-\dfrac{D}{2\sqrt{3}}\right]^{-1} \end{array}\right\} \text{infinite } \langle 111 \rangle \text{ stress ,} \tag{14b}$$

$$\left.\begin{array}{l} m_l/m_0=\left[A+B\eta_1/2+\dfrac{\sqrt{3}}{2}D\eta_2\right]^{-1} \\ m_{t1}/m_0=\left[A+B\eta_1/2-\dfrac{\sqrt{3}}{2}D\eta_2\right]^{-1} \\ m_{t2}/m_0=(A-B\eta_1)^{-1} \end{array}\right\} \text{infinite } \langle 110 \rangle \text{ stress ,} \tag{14c}$$

where m_0 is the free-electron mass,

$$\eta_1=\left[\frac{1}{1+3\beta^2}\right]^{1/2} , \quad \eta_2=\left[\frac{\beta^2}{1+3\beta^2}\right]^{1/2} ,$$

and

$$\beta=\frac{d(C_{11}-C_{12})}{2\sqrt{3}bC_{44}}=\frac{E_{\epsilon\epsilon}/\sigma \text{ for } \langle 111 \rangle}{E_{\epsilon\epsilon}/\sigma \text{ for } \langle 001 \rangle}$$

is the splitting anisotropy parameter. The optical mass [from Eqs. (11) and (12)] and density-of-states mass are

$$\left.\begin{array}{l} m_{oh}/m_0=A^{-1} \\ m_{dh}/m_0=(m_{t1}m_{t2}m_l)^{1/3}/m_0 \end{array}\right\} \text{infinite stress ,} \tag{15}$$

with the transverse and longitudinal components given by Eq. (14).

III. RESULTS

It can easily be seen from Eqs. (1) and (2) that the valence-band dispersion scales with stress, sug-

gesting the introduction of reduced units $E' \equiv -E/\sigma$ and $k' \equiv k/\sqrt{-\sigma}$. The masses then are functions only of E', not of energy and stress independently.

Local and integrated density-of-states masses were calculated versus E' for the $|M_J| = \frac{1}{2}$ and $\frac{3}{2}$ bands using Eqs. (5) and (8). The results for stresses along the principal crystallographic directions $\langle 001 \rangle$, $\langle 110 \rangle$, and $\langle 111 \rangle$ are shown in Fig. 1 for Ge and in Fig. 2 for Si. The local masses in Fig. 1(c) were published previously[3] and are reproduced here for completeness. The integrated masses smooth out the more rapid changes in the local masses, including the structure in the local $\langle 111 \rangle$ $|M_J| = \frac{1}{2}$ masses. Note that the local and integrated masses become equal at infinite stress ($E'=0$) and at zero stress ($E'=\infty$, indicated by arrows in the figures). The values obtained at zero stress were $m_{dHH} = 0.3460 m_0$, $m_{dLH} = 0.04231 m_0$ for Ge and $m_{dHH} = 0.5230 m_0$, $m_{dLH} = 0.1549 m_0$ for Si, in agreement with those calculated by Brinkman and Rice.[18] In addition, the calculated

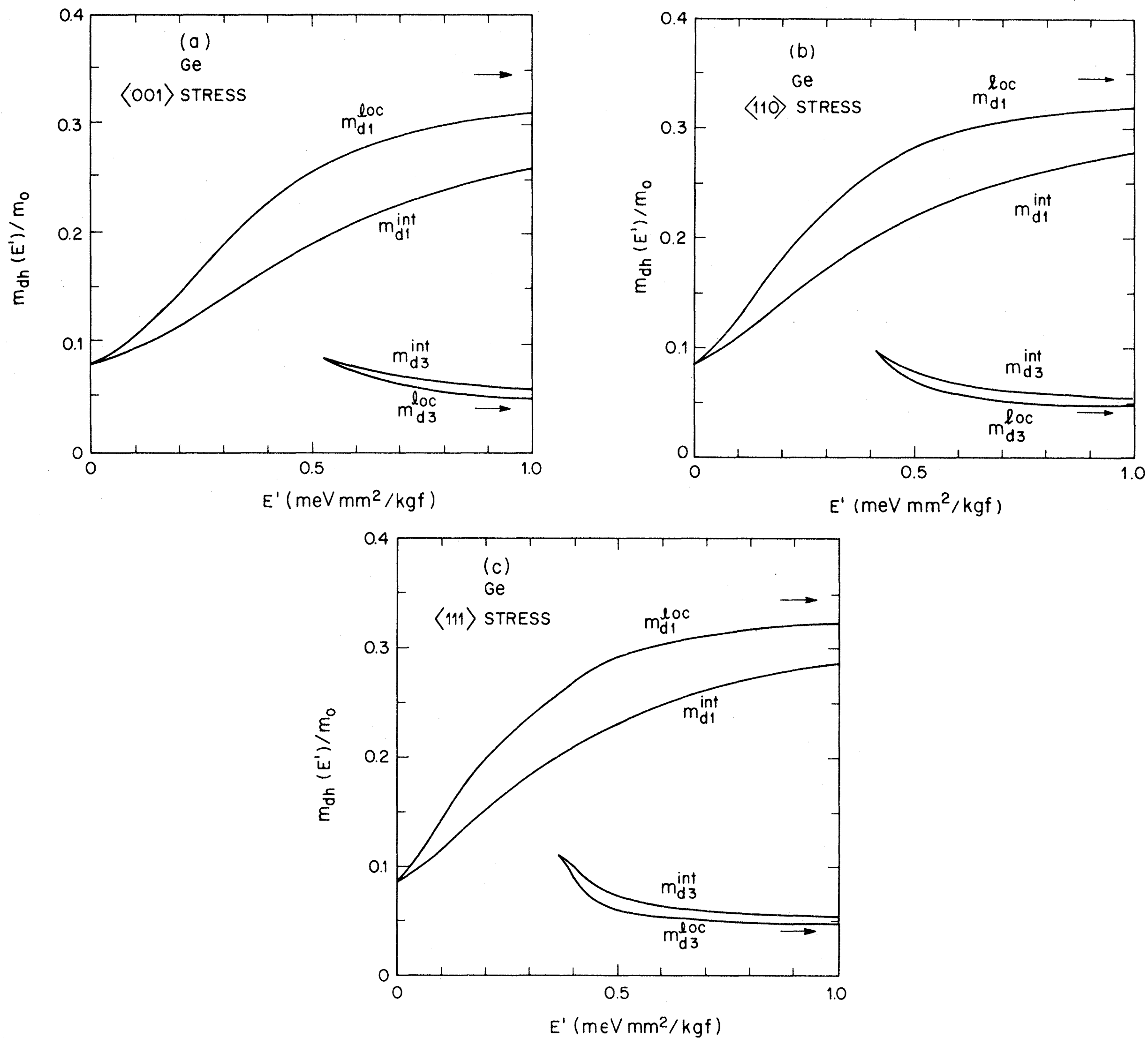

FIG. 1. Local and integrated density-of-states masses for the valence bands corresponding to $|M_J| = \frac{1}{2}$ and $\frac{3}{2}$ in stressed Ge as a function of reduced energy $E' = -E/\sigma$. The 2's have been suppressed. The arrows indicate zero-stress values. (a) $\langle 001 \rangle$, (b) $\langle 110 \rangle$, and (c) $\langle 111 \rangle$ stress.

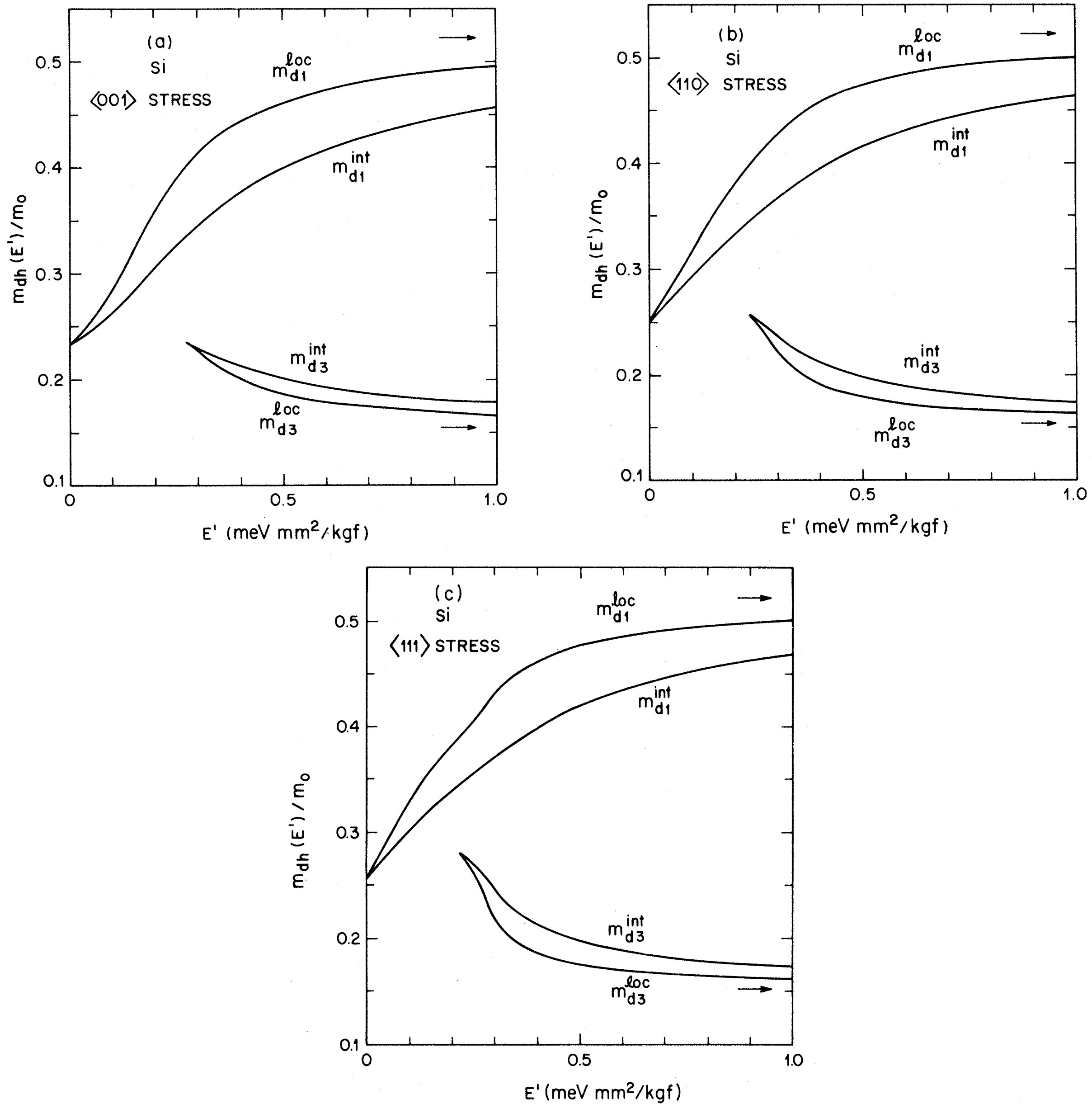

FIG. 2. Local and integrated density-of-states masses for the valence bands corresponding to $|M_J|=\frac{1}{2}$ and $\frac{3}{2}$ in stressed Si as a function of reduced energy $E'=-E/\sigma$. The 2's have been suppressed. The arrows indicate zero-stress values. (a) $\langle 001\rangle$, (b) $\langle 110\rangle$, and (c) $\langle 111\rangle$ stress.

infinite-stress values agree with those obtained from Eq. (15), as they should.

Longitudinal and transverse components of the $|M_J|=\frac{1}{2}$ and $\frac{3}{2}$ optical masses were also calculated, using Eqs. (9) and (10). Results for $\langle 001\rangle$, $\langle 110\rangle$, and $\langle 111\rangle$ stresses are shown in Fig. 3 for Ge and in Fig. 4 for Si. For the $|M_J|=\frac{1}{2}$ band the transverse optical masses are always larger than the longitudinal optical mass, while the reverse is true for the $|M_J|=\frac{3}{2}$ band. The mass anisotropies, represented by the ratios m_{o1t}/m_{o1l} and m_{o3l}/m_{o3t}, are greater for the $\langle 110\rangle$ and $\langle 111\rangle$ directions than for $\langle 001\rangle$. The $|M_J|=\frac{3}{2}$ mass anisotropy for $\langle 110\rangle$ and $\langle 111\rangle$ undergoes a remarkable change for E' just greater than $-E_{\mathrm{spl}}^{h}/\sigma$. This would be very interesting to observe experimentally. Note, however, that the rapid change occurs when this band has relatively

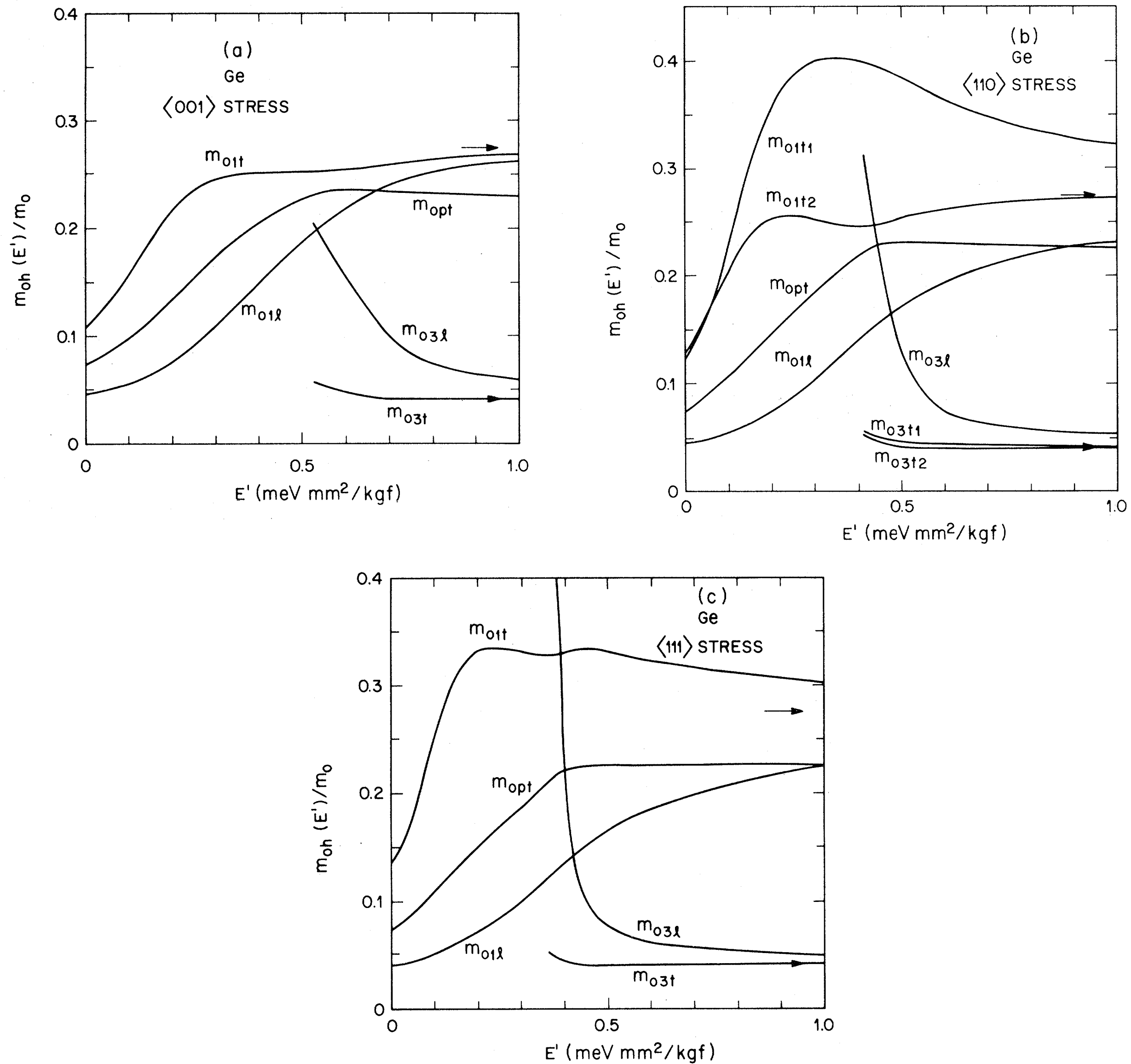

FIG. 3. Transverse and longitudinal components of optical masses for the $|M_J|=\frac{1}{2}$ and $\frac{3}{2}$ valence bands in stressed Ge as a function of reduced energy $E'=-E/\sigma$. The 2's have been suppressed. The total optical mass is also shown. The arrows indicate zero-stress values for the heavy and light masses. (a) ⟨001⟩, (b) ⟨110⟩, and (c) ⟨111⟩ stress.

low population. The longitudinal and transverse components become equal at zero stress, as a consequence of the cubic symmetry of the lattice. These zero-stress values indicated by arrows in the figures are $m_{oHH}=0.2754m_0$, $m_{oLH}=0.04210m_0$ for Ge and $m_{oHH}=0.4195m_0$, $m_{oLH}=0.1497m_0$ for Si. The calculated infinite-stress values agree with those obtained from Eq. (14), as they should.

The total optical masses m_{oh}, or $m_{\rm opt}$, averaged over longitudinal and transverse components as well as $|M_J|$ values according to Eqs. (11)–(13), are also shown in Figs. 3 and 4. It is notable that $m_{\rm opt}$ is not a monotonic function of E' but has a maximum for $E'\sim0.5$ in Ge and $E'\sim0.3$ in Si, slightly greater than $-E^h_{\rm spl}/\sigma$. Since the mass m_{o1} is monotonic, the maximum in $m_{\rm opt}$ occurs as the $|M_J|=\frac{3}{2}$ contribution becomes more important. The values obtained for zero stress are $m_{\rm opt}=0.2244m_0$ for Ge and $m_{\rm opt}=0.3356m_0$ for Si.

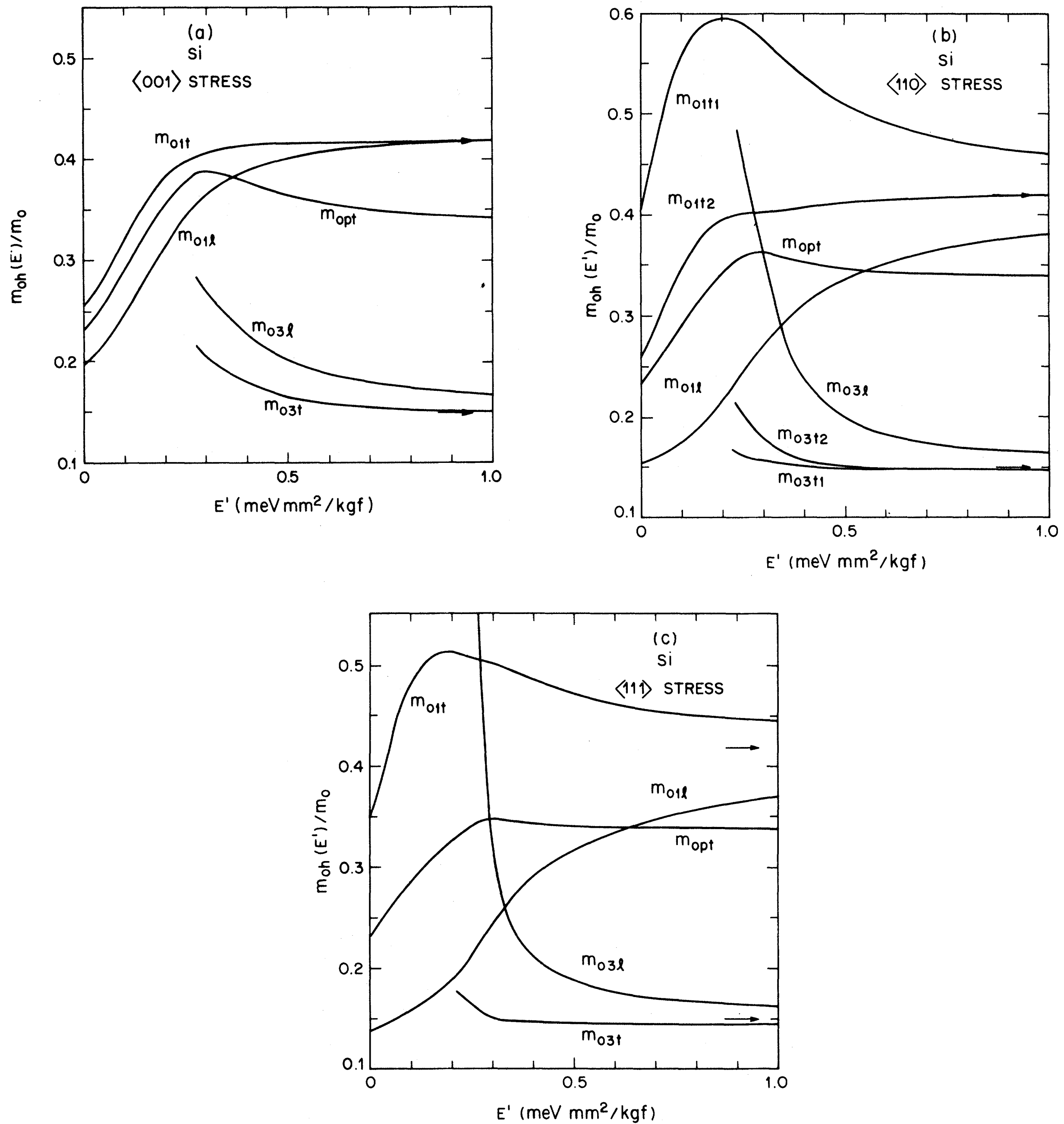

FIG. 4. Transverse and longitudinal components of optical masses for the $|M_J|=\frac{1}{2}$ and $\frac{3}{2}$ valence bands in stressed Si as a function of reduced energy $E'=-E/\sigma$. The 2's have been suppressed. The total optical mass is also shown. The arrows indicate zero-stress values for the heavy and light masses. (a) ⟨001⟩, (b) ⟨110⟩, and (c) ⟨111⟩ stress.

The curves of Figs. 1–4 can easily be fitted with analytic formulas to facilitate further calculations.[7,9] Tables of values for all the mass components may be obtained from the author. It may be anticipated from the figures that it is important to include the energy dependences of the masses at stresses beyond the stress at which the $|M_J|=\frac{3}{2}$ band becomes depopulated. An example is given in the next section.

IV. DISCUSSION

As an illustration of one use of the energy- and stress-dependent masses defined in Sec. II, consider the luminescence line shape for the electron-hole liquid in stressed Ge or Si. For an allowed indirect transition with an energy-independent matrix element, the luminescence intensity as a function of photon energy $h\nu$ is given by the joint density of occupied electron and hole states. For a single conduction band and valence band,[19,20]

$$I(h\nu)=I_0\int_0^\infty dE_e\int_0^\infty dE_h D_e(E_e)D_h(E_h)(1+e^{[E_e-E_F^e(T)]/kT})^{-1}(1+e^{[E_h-E_F^h(T)]/kT})^{-1} \times\delta(h\nu-E_e-E_h+\hbar\omega_{ph}-E_{BB}) , \quad (16)$$

where $E_{e(h)}$ and $E_F^{e(h)}$ are the electron (hole) energy and Fermi energy, E_{BB} is the bottom of the band within the EHL, $\hbar\omega_{ph}$ is the energy of the phonon emitted to conserve momentum in the indirect transition, and the densities of states are given by Eqs. (4a) and (4b) for electrons and holes.

In stressed Ge or Si the valence bands are split by an energy E_{spl}^h and the conduction bands are split by an energy E_{spl}^e, with ν_1 electron valleys below the other ν_2 electron valleys. The contributions must be added for transitions between each pair of bands. The integral over E_e can be performed immediately. Thus

$$I(E_{BB}-\hbar\omega_{ph}+h\nu')=I_0\int_0^{h\nu'}(R_{e1}+R_{e2})(R_{h1}+R_{h3})dE_h , \quad (17a)$$

where

$$R_{e1}=\nu_1 m_{de}^{3/2}(h\nu'-E_h)^{1/2}(1+e^{[h\nu'-E_h-E_F^e(T)]/kT})^{-1} \quad (17b)$$

$$R_{e2}=\begin{cases}0, & h\nu'-E_h\le E_{spl}^e\\ \nu_2 m_{de}^{3/2}(h\nu'-E_{spl}^e-E_h)^{1/2}(1+e^{[h\nu'-E_h-E_F^e(T)]/kt})-1, & h\nu'-E_h>E_{spl}^e\end{cases} \quad (17c)$$

$$R_{h1}=m_{d1}^{3/2}(E_h')E_h^{1/2}(1+e^{[E_h-E_F^h(T)]/kT})^{-1} \quad (17d)$$

$$R_{h3}=\begin{cases}0, & E_h\le E_{spl}^h\\ m_{d3}^{3/2}(E_h')(E_h-E_{spl}^h)^{1/2}(1+e^{[E_h-E_F^h(T)]/kT})^{-1}, & E_h>E_{spl}^h .\end{cases} \quad (17e)$$

Here $h\nu'=h\nu-E_{BB}+\hbar\omega_{ph}$, m_{de} is the density-of-states electron mass, the local density-of-states hole masses are used, $E_h'=-E_h/\sigma$, and some constants have been absorbed into I_0.

The importance of including the nonparabolicity of the hole bands in the luminescence line shape is illustrated in Fig. 5. The solid curve is a line shape calculated for $T=1.4$ K and $-\sigma=55$ kgf/mm^2 along $\langle 001\rangle$ in Si ($\nu_1=2$, $\nu_2=4$, $m_{de}=0.3216m_0$). The electron-hole pair density was chosen to be $n=5.53\times10^{17}$ cm^{-3}, corresponding to electron and hole Fermi energies $E_F^e=4.81$ meV and $E_F^h=8.50$ meV. The resulting full-width-at-half-maximum linewidth was $\Delta E=6.8$ meV. The energy-dependent density-of-states mass from Fig. 2(a) was used in the calculation. Note that $-E_F^h/\sigma=0.155$ meV mm^2/kgf, which is well below the value $-E_{spl}^h/\sigma=0.272$ meV mm^2/kgf for this stress direction (see Table I). Thus the stress is well above the critical stress required to depopulate the $|M_J|=\frac{3}{2}$ band.

In the absence of information about the energy dependence of the hole density-of-states mass it would seem reasonable to fit an experimental spectrum for such a high stress to a spectrum calculated using the infinite-stress mass. The dashed curve in Fig. 5 was calculated in that way, with the density adjusted to give the same linewidth $\Delta E=6.8$ meV. In this case $E_F^e=3.74$ meV, $E_F^h=8.15$ meV, and the density $n=3.79\times10^{17}$ cm^{-3}. With the incorrect use of the infinite-stress hole mass, the density is underestimated in this example by nearly $\frac{1}{3}$, even though the stress is high enough to depopulate the $|M_J|=\frac{3}{2}$ band. If the infinite-stress mass is used to fit a spectrum for a lower stress, the deduced density will have a larger error.

It is clear from this example that it is necessary to use the energy-dependent hole masses to analyze

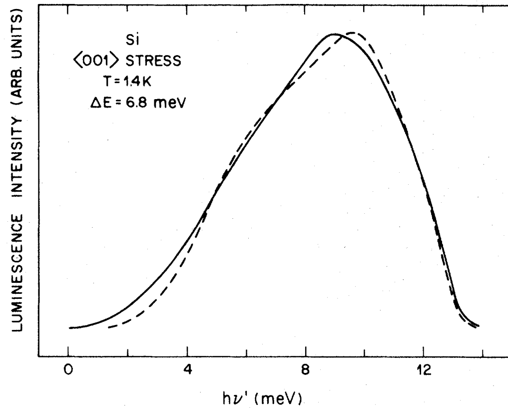

FIG. 5. Theoretical luminescence line shapes for the electron-hole liquid in ⟨001⟩-stressed Si with densities chosen to give a full width at half maximum $\Delta E = 6.8$ meV ($T = 1.4$ K). Solid curve: uses energy-dependent density-of-states hole mass from Fig. 2(a), with $-\sigma = 55$ kgf/mm^2 and $n = 5.53 \times 10^{17}$ cm^{-3}. Dashed curve: uses infinite-stress hole mass and $n = 3.79 \times 10^{17}$ cm^{-3}. The dashed curve has been shifted so its half maximum points agree with those of the solid curve.

luminescence line shapes. In addition to the (possibly large) errors in deduced densities, the entire line shape changes. Clearly the *quality* of the line-shape fit should change (hopefully, improve) when the correct theoretical line shape is used.

ACKNOWLEDGMENTS

The author would like to thank R. S. Markiewicz for assistance and advice during the initial phase of the calculations. The work performed at the University of California and at Lawrence Berkeley Laboratory was supported in part by the Director, Office of Energy Research, Office of Basic Energy Sciences, Material Sciences Division of the U. S. Department of Energy under Contract No. W-7405-ENG-48.

*Present address: Xerox Palo Alto Research Center, Palo Alto, California 94304.

[1]For a review and further references, see the articles by T. M. Rice and by J. C. Hensel, T. G. Phillips, and G. A. Thomas, in *Solid State Physics,* edited by H. Ehrenreich, F. Seitz, and D. Turnbull (Academic, New York, 1977), Vol. 32.

[2]R. S. Markiewicz and S. M. Kelso, Solid State Commun. 25, 275 (1978).

[3]J. P. Wolfe, R. S. Markiewicz, S. M. Kelso, J. E. Furneaux, and C. D. Jeffries, Phys. Rev. B 18, 1479 (1978).

[4]L. Liu, Solid State Commun. 25, 805 (1978).

[5]G. Kirczenow and K. S. Singwi, Phys. Rev. B 19, 2117 (1979).

[6]L. Liu and Lu Sun Liu, Solid State Commun. 27, 801 (1978).

[7]S. M. Kelso, thesis, University of California, Berkeley 1979 (unpublished).

[8]G. Kirczenow and K. S. Singwi, Phys. Rev. B 21, 3597 (1980); G. Kirczenow, *ibid.* 23, 1902 (1981), and references therein.

[9]S. M. Kelso (unpublished).

[10]G. E. Pikus and G. L. Bir, Fiz. Tverd. Tela (Leningrad) 1, 1642 (1959) [Sov. Phys.—Solid State 1, 1502 (1959)].

[11]I. Balslev, Phys. Rev. 143, 636 (1966).

[12]G. Dresselhaus, A. F. Kip, and C. Kittel, Phys. Rev. 98, 368 (1955).

[13]J. C. Hensel and G. Feher, Phys. Rev. 129, 1041 (1963).

[14]J. C. Hensel and K. Suzuki, Phys. Rev. B 9, 4219 (1974).

[15]Formulas are given here in terms of stiffness constants C_{ij} rather than compliance constants S_{ij}, since experimental values for the C_{ij} are available (see Table I). Traditionally there has been some confusion over tensor vs engineering notation for these quantities. We assume that the same notation has been used in all cases, so that $S_{11} - S_{12} = (C_{11} - C_{12})^{-1}$, $S_{11} + 2S_{12} = (C_{11} + 2C_{12})^{-1}$, and $S_{44} = (C_{44})^{-1}$.

[16]J. H. Rose, H. B. Shore, and T. M. Rice, Phys. Rev. B 17, 752 (1978).

[17]B. Lax and J. G. Mavroides, Phys. Rev. 100, 1650 (1955).

[18]W. F. Brinkman and T. M. Rice, Phys. Rev. B 7, 1508 (1973).

[19]Ya. E. Pokrovskii, A. Kaminskii, and K. I. Svistunova, in *Proceedings of the Tenth International Conference on the Physics of Semiconductors, Cambridge,* edited by S. P. Keller, J. C. Hensel, and F. Stern (USAEC, Division of Technical Information, Oak Ridge, Tenn., 1970), p. 504.

[20]C. Benôit à la Guillaume and M. Voos, Phys. Rev. B 7, 1723 (1973).